

Non-thermal Production of Minimal Dark Matter via Right-handed Neutrino Decay

Mayumi Aoki^{1*}, Takashi Toma^{2†}, Avelino Vicente^{3,4‡}

¹*Institute for Theoretical Physics, Kanazawa University, Kanazawa 920-1192, Japan*

²*Laboratoire de Physique Théorique, CNRS - UMR 8627,
Université de Paris-Sud 11, F-91405 Orsay Cedex, France*

³*IFPA, Dep. AGO, Université de Liège, Bat B5, Sart-Tilman B-4000 Liège 1, Belgium*

⁴*Instituto de Física Corpuscular (CSIC-Universitat de València),
Apdo. 22085, E-46071 Valencia, Spain*

Abstract

Minimal Dark Matter (MDM) stands as one of the simplest dark matter scenarios. In MDM models, annihilation and co-annihilation processes among the members of the MDM multiplet are usually very efficient, pushing the dark matter mass above $\mathcal{O}(10)$ TeV in order to reproduce the observed dark matter relic density. Motivated by this little drawback, in this paper we consider an extension of the MDM scenario by three right-handed neutrinos. Two specific choices for the MDM multiplet are studied: a fermionic $SU(2)_L$ quintuplet and a scalar $SU(2)_L$ septuplet. The lightest right-handed neutrino, with tiny Yukawa couplings, never reaches thermal equilibrium in the early universe and is produced by freeze-in. This creates a link between dark matter and neutrino physics: dark matter can be non-thermally produced by the decay of the lightest right-handed neutrino after freeze-out, allowing to lower significantly the dark matter mass. We discuss the phenomenology of the non-thermally produced MDM and, taking into account significant Sommerfeld corrections, we find that the dark matter mass must have some specific values in order not to be in conflict with the current bounds from gamma-ray observations.

*mayumi@hep.s.kanazawa-u.ac.jp

†takashi.toma@th.u-psud.fr

‡Avelino.Vicente@ulg.ac.be

1 Introduction

The identity of the Dark Matter (DM) that makes up about 25% of the energy content of the universe is one of the most important open problems in (astro-)particle physics. Lots of candidates have been proposed under the assumption that DM is made of particles. The most popular options include Weakly Interacting Massive Particles (WIMPs), axions, gravitinos and asymmetric dark matter. In particular, WIMPs are theoretically well-motivated candidates since the present relic density of DM can be reproduced by thermal production in the early universe with an electroweak scale DM mass and an annihilation cross section $\langle\sigma v\rangle \approx 3 \times 10^{-26} \text{ cm}^3/\text{s}$, in the typical range for a particle with weak interactions. This intriguing coincidence, usually called *the WIMP miracle*, has triggered a massive exploration of WIMP DM scenarios, with detailed studies of their phenomenological implications and dedicated experimental searches for DM in the form of WIMPs in colliders as well as in direct and indirect detection experiments.

In scenarios with electroweak scale DM, a discrete symmetry is often imposed in order to stabilize the DM candidate. Although this symmetry is usually introduced *by hand*, many theoretical justifications are known. For instance, this symmetry can be seen as a remnant after the spontaneous breaking of a larger symmetry group. Many proposals in this direction exist, based on global [1–3] or gauge symmetries [4–6], some of them linked to flavor symmetries [7, 8]. A completely different approach is to consider that the origin of this symmetry is accidental. If a large multiplet of the $SU(2)_L$ gauge symmetry of the Standard Model (SM) is introduced, an accidental \mathbb{Z}_2 symmetry may appear due to the restrictions imposed by gauge invariance and renormalizability. This is the so-called *Minimal Dark Matter* (MDM) approach [9], a popular scenario with some recent works [10–14].

There is, however, a generic drawback in MDM scenarios: the components of the large $SU(2)_L$ multiplets are generally required to be nearly degenerate. The origin of this mass degeneracy is easy to understand. First of all, in some MDM models this is actually predicted, since the mass splittings among components of the large $SU(2)_L$ multiplets only appear at the one-loop level [15, 16]. When this is not the case, and large mass splittings can in principle be obtained, one must face two problems. First, the large $SU(2)_L$ multiplets contribute to electroweak precision observables (EWPO) through the STU oblique parameters and, in order to be compatible with the current experimental measurements, one typically requires small mass splittings [17, 18]. And second, the mass splittings must be induced by Higgs-DM-DM couplings for scalar DM, which are required to be small in order to suppress the elastic scattering with nuclei via Higgs exchange and be compatible with direct detection constraints (see for example [19]). As a result of this degeneracy, all members of the multiplet will be in thermal equilibrium during freeze-out, co-annihilating very efficiently with the DM particles and strongly reducing the DM relic density. In order to reproduce the relic density measured by Planck, $\Omega_{\text{DM}} h^2 = 0.1186 \pm 0.0020$ at 68% Confidence Level (CL) [20], this implies a heavy DM

particle. In fact, once Sommerfeld corrections are included [21], the DM mass is typically found to be about $\mathcal{O}(10)$ TeV. Although perfectly plausible, this is not very attractive from a phenomenological point of view.

Another open problem that calls for physics beyond the SM is the existence of non-zero neutrino masses and mixings, as established by neutrino oscillation experiments. Many extensions of the SM have been proposed to address this issue. The energy scale for the new states responsible for neutrino mass generation can be either very high, potentially relating neutrino masses to unification, or low (TeV scale or below). In the latter case, the existence of new physics at low energies leads to interesting phenomenological perspectives, within the reach of current collider and low-energy experiments. Furthermore, many neutrino mass models include DM candidates, although an interplay between these two fundamental issues is often missing.

In this paper, we consider a very economical extension of the MDM scenario. In addition to the multiplet containing the DM particle, three right-handed neutrino singlets are introduced. No additional symmetry for DM stabilization is required due to an accidental \mathbb{Z}_2 symmetry resulting from the gauge invariant renormalizable interactions of the DM multiplet. The right-handed neutrinos play two roles in this model. First, neutrino masses are induced at tree-level with the standard Type-I Seesaw mechanism [22–26], and second, the out-of-equilibrium decay of the right-handed neutrinos leads to non-thermal production of DM, allowing one to compensate the strong effect of co-annihilations and lower the DM mass below the TeV scale.¹ This setup will be illustrated with two specific examples: a model with a fermionic quintuplet and a model with a scalar septuplet, in both cases with vanishing hypercharge.² The number of physical parameters in both models is limited and many experimental constraints exist. As a result of this, the setup is very predictive and will definitely be tested in future experiments.

The rest of the paper is organized as follows: in Sec. 2 we introduce the setup, comment on the degeneracy among the members of the MDM multiplet and discuss the mechanism responsible for neutrino mass generation. The DM phenomenology of these models is explored in Sec. 3, where we present the main results of this paper. The most relevant constraints in our scenario are discussed in Sec. 4 and, finally, we summarize and present the main conclusions of the paper in Sec. 5.

2 The Models

2.1 New particles and interactions

We consider an extension of the SM by three right-handed neutrinos N_i ($i = 1 - 3$) and a $SU(2)_L$ multiplet χ which is either a quintuplet fermion or a septuplet scalar, as

¹Non-thermal production of Wino DM (triplet) has been discussed in Ref. [27].

²Septuplets with hypercharge $Y = 2$ have also been considered in Refs. [28, 29], although with a completely different motivation: the extended model keeps the ρ -parameter as 1 at tree-level.

	N_i	χ
$SU(2)_L$	1	5 (7)
$U(1)_Y$	0	0
spin	1/2	1/2 (0)

Table 1: New particle content and charge assignment in the two models under consideration. Here $i = 1, 2, 3$. The first model introduces a quintuplet fermion, whereas the second introduces a septuplet scalar, in both cases with $Y = 0$.

summarized in Tab. 1. The quintuplet fermion and the septuplet scalar can be denoted by the vectors

$$\chi \equiv i \begin{pmatrix} +\chi^{++} \\ +\chi^+ \\ -\chi^0 \\ +\chi^- \\ +\chi^{--} \end{pmatrix}, \quad \chi \equiv i \begin{pmatrix} +\chi^{+++} \\ +\chi^{++} \\ +\chi^+ \\ -\chi^0 \\ -\chi^- \\ +\chi^{--} \\ -\chi^{---} \end{pmatrix}. \quad (1)$$

The prefactor i and the sign for each component are taken in order to satisfy $\chi^c = \chi$ where χ^c denote charge conjugation of the field χ . Further details about products of $SU(2)$ multiplets are given in Appendix A. The kinetic and Yukawa Lagrangians of the new particles are given by

$$\mathcal{L} = \mathcal{L}_K^{\text{MDM}} + \frac{1}{2} \overline{N}_i^c (i\not{\partial} - m_{N_i}) N_i - (y_{i\alpha}^\nu \phi \overline{N}_i P_L L_\alpha + \text{H.c.}), \quad (2)$$

where $\mathcal{L}_K^{\text{MDM}}$ is the kinetic term of the multiplet given by

$$\mathcal{L}_K^{\text{MDM}} = \begin{cases} \frac{1}{2} \overline{\chi^c} (i\not{\partial} - m_\chi) \chi & \text{for the quintuplet fermion,} \\ \frac{1}{2} (D_\mu \chi) (D^\mu \chi) & \text{for the septuplet scalar.} \end{cases} \quad (3)$$

The covariant derivative is defined by $D_\mu \equiv \partial_\mu + ig_2 W_\mu^a T^a$ with the $SU(2)_L$ gauge coupling g_2 , gauge field W_μ^a and generator T^a ($a = 1, 2, 3$). Note that Eq. (2) is written in the basis in which the right-handed neutrino Majorana mass term is diagonal. From the Lagrangian, one can see that the right-handed neutrinos dominantly interact with the longitudinal mode of gauge bosons W^\pm and Z , while the MDM multiplet χ interacts with the transverse mode. The scalar potential for the model with the quintuplet fermion is exactly the same as in the SM ($\mathcal{V}_5 = \mathcal{V}_{\text{SM}}$), whereas that for the septuplet scalar model is

$$\mathcal{V}_7 = -\mu_\phi^2 |\phi|^2 + \frac{\mu_\chi^2}{2} \chi^2 + \frac{\lambda_\phi}{4} |\phi|^4 + \sum_{k=1}^2 \frac{\lambda_{\chi k}}{4!} [\chi^4]_k + \frac{\lambda_{\phi\chi}}{2} |\phi|^2 \chi^2, \quad (4)$$

where ϕ is the SM Higgs doublet with hypercharge $Y_\phi = 1/2$. In the following, the scalar coupling $\lambda_{\phi\chi}$ is assumed to be small, as in Ref. [9].

Several comments about the scalar potential in Eq. (4) are in order. First, we note that in some cases various singlet contractions of $SU(2)_L$ higher dimensional representations are possible. For example, four kinds of singlets can be constructed for the χ^4 term. However only two of them are independent. This is denoted with a summation in Eq. (4). Furthermore, there is no septuplet cubic term χ^3 , since the singlet obtained by contracting three septuplets is completely anti-symmetric: $\mathbf{7} \otimes \mathbf{7} \otimes \mathbf{7} \supset \mathbf{1}_A$. As a result, an accidental \mathbb{Z}_2 symmetry appears, under which the septuplet χ is odd and the rest of the fields even. The same accidental symmetry appears for the quintuplet fermion as well. Therefore, the lightest state contained in the quintuplet or septuplet will be stable and a DM candidate is automatically included in the model without any additional symmetry.³ One should note that for the septuplet scalar, the dimension 5 operator $\chi^3|\phi|^2/\Lambda$, where Λ is the energy scale at which the operator is induced, leads to the decay of the DM candidate at one-loop level and is not forbidden by any symmetry. As it has been recently discussed in Ref. [30], $\Lambda \gtrsim 10^{20}$ GeV is necessary for $m_\chi \sim 10$ TeV in order to obtain a DM lifetime longer than the age of the universe, $\tau_U \sim 10^{18}$ s. Moreover, pairs of gauge bosons $\gamma\gamma$, γZ , ZZ and W^+W^- are produced by the DM decays, and these are constrained by gamma-ray experiments. One finds that the DM lifetime should be roughly $\tau_\chi \gtrsim 10^{27}$ s to evade them. This corresponds to $\Lambda \gtrsim 10^{25}$ GeV which is much larger than the Planck scale. In contrast, there is no possible 5 dimensional operator for the quintuplet fermion case [30]. The possible 6 dimensional operators are $\chi L_\alpha |\phi|^2 \phi / \Lambda^2$ and $\chi \sigma^{\mu\nu} L_\alpha \phi W_{\mu\nu} / \Lambda^2$, where $W_{\mu\nu}$ is the field strength tensor for the $SU(2)_L$ gauge group. For such 6 dimensional operators, a DM lifetime long enough to satisfy the gamma-ray constraints can be achieved with $\Lambda = 10^{15}$ GeV. Thus, the quintuplet fermion DM candidate would be stable even if one includes non-renormalizable operators.

Finally, lepton number is softly broken by the Majorana mass term of the right-handed neutrinos. As a consequence, neutrinos acquire Majorana masses through the canonical type-I seesaw mechanism, as we will see below.

2.2 Mass degeneracy within the MDM multiplets

After electroweak symmetry breaking, only the SM Higgs doublet gets a non-zero VEV, $\phi^0 = \langle \phi \rangle + h/\sqrt{2}$. The Higgs boson mass is given by $m_h^2 = \lambda_\phi \langle \phi \rangle^2$ and all the components of the multiplet χ have the same mass m_χ at tree-level. The mass m_χ is given by the bare mass in Eq. (3) for the quintuplet fermion and $m_\chi^2 = \mu_\chi^2 + \lambda_{\phi\chi} \langle \phi \rangle^2$ for the septuplet scalar. However, a mass difference is induced at the one-loop level. Given two components of the MDM multiplets with electric charges Q and Q' , the one-loop

³For the septuplet scalar, we will assume that the vacuum of the theory is such that no other scalar field besides the usual Higgs doublet has a vacuum expectation value (VEV). This guarantees that the accidental \mathbb{Z}_2 symmetry remains after electroweak symmetry breaking.

induced mass splitting is computed to be

$$m_Q - m_{Q'} = (Q^2 - Q'^2) \frac{m_\chi}{4\pi} \left[\alpha_W \left\{ f\left(\frac{m_W}{m_\chi}\right) - f\left(\frac{m_Z}{m_\chi}\right) \right\} + \alpha_{\text{em}} \left\{ f\left(\frac{m_Z}{m_\chi}\right) - f(0) \right\} \right], \quad (5)$$

where $\alpha_W = g_2^2/(4\pi)$, $\alpha_{\text{em}} = e^2/(4\pi)$ and the function $f(z)$ is defined as

$$f(z) = 2 \int_0^1 (1+x) \log\left((1-x)z^2 + x^2\right) dx, \quad (6)$$

for the quintuplet fermion and

$$f(z) = -\frac{1}{2} \int_0^1 \left(6(1-x)z^2 + 9x^2 - 4x - 4\right) \log\left((1-x)z^2 + x^2\right) dx, \quad (7)$$

for the septuplet scalar. The septuplet scalar not only has $SU(2)_L$ gauge interactions, but also scalar couplings $\lambda_{\chi k}$ and $\lambda_{\phi\chi}$ in the potential. These couplings also give a correction to the scalar masses. However, the mass corrections for all the components of the septuplet are exactly the same and no mass difference is generated in this way. We note that, although it may seem that our results differ from those in Ref. [9], we have checked explicitly that our expressions in Eqs. (5)-(7) are consistent with those in this reference.

Inspection of Eqs. (5)-(7) reveals some relevant features of the mass degeneracy within the MDM multiplets. For light multiplets ($m_\chi \ll m_W, m_Z$) the corrections are negligible for quintuplets but can reach a few GeV in the case of septuplets. Then, as the multiplet mass increases, the splitting in both cases approaches a common value. In fact, in the $m_\chi \rightarrow \infty$ limit one finds

$$m_Q - m_{Q'} = (Q^2 - Q'^2) \alpha_W m_W \sin^2\left(\frac{\theta_W}{2}\right) \approx (Q^2 - Q'^2) \times 166 \text{ MeV}, \quad (8)$$

in both MDM scenarios (quintuplet and septuplet). Therefore, although the behavior of the loop function $f(z)$ is different for low m_χ values, it is the same for $m_\chi \gg m_W, m_Z$, leading to a *universal* splitting in case of heavy MDM multiplets. This universality can be used to estimate the resulting splitting at the two-loop level. The mass splitting between the singly charged and neutral components of a triplet fermion was calculated at the two-loop level in Ref. [31], finding the value 164.4 MeV in the limit of an infinitely heavy triplet. Given the universality of this limit, we expect the same conclusion to hold in our two MDM scenarios. Finally, we also note that the previous expressions imply that the neutral component χ^0 , is the lightest of the components of the MDM multiplet, thus becoming a viable DM candidate.

2.3 Neutrino mass matrix

The Lagrangian relevant for the generation of neutrino masses is

$$\mathcal{L}_\nu = - (m_D)_{i\alpha} \bar{N}_i P_L \nu_\alpha - \frac{m_{N_i}}{2} \bar{N}_i^c N_i + \text{H.c.}, \quad (9)$$

where $(m_D)_{i\alpha} = y'_{i\alpha} \langle \phi \rangle$ is the usual neutrino Dirac mass term. Assuming $(m_D)_{i\alpha} \ll m_{N_i}$, the light neutrinos acquire Majorana masses via the canonical type-I seesaw mechanism,

$$m_\nu \approx -m_D^T m_N^{-1} m_D. \quad (10)$$

The light neutrino mass matrix in Eq. (10) is diagonalized by the Pontecorvo-Maki-Nakagawa-Sakata matrix U_{PMNS} as

$$U_{\text{PMNS}}^T m_\nu U_{\text{PMNS}} = \begin{pmatrix} m_1 & 0 & 0 \\ 0 & m_2 & 0 \\ 0 & 0 & m_3 \end{pmatrix}. \quad (11)$$

It is common to use the Casas-Ibarra parametrization to write the neutrino Yukawa coupling y^ν as [32]

$$y^\nu = \frac{1}{\langle \phi \rangle} D_{\sqrt{m_N}} R D_{\sqrt{m}} U_{\text{PMNS}}^\dagger, \quad (12)$$

where $D_{\sqrt{m_N}} = \text{diag}(\sqrt{m_{N_i}})$, $D_{\sqrt{m}} = \text{diag}(\sqrt{m_i})$, R is an orthogonal matrix ($R^T R = R R^T = \mathbb{1}$) and the extra phase of the Yukawa coupling has been absorbed into the fields.

As we will see below, non-thermal production of DM requires right-handed neutrinos with masses $m_{N_i} \gtrsim 5$ TeV. Therefore, the Yukawa couplings of the right-handed neutrinos participating in the generation of the light neutrino masses will be of the order of $y^\nu \gtrsim 10^{-6}$ in order to obtain an appropriate neutrino mass scale.

3 Non-thermal production of Minimal Dark Matter

The most recent measurement of the DM relic density by the Planck Collaboration is $\Omega_{\text{DM}} h^2 = 0.1186 \pm 0.0020$ at 68% CL [20]. In this section we will study the implications of this measurement for our setup, where the lightest neutral component of the MDM multiplet χ^0 , is the DM candidate due to the accidental \mathbb{Z}_2 symmetry.

A DM particle with $SU(2)_L$ gauge interactions and a mass larger than the W boson mass would mainly annihilate into a pair of gauge bosons, typically implying a strong reduction of the relic density. Thus, in the case of the MDM scenario with a large dimensional representation [9], the DM mass has to be above several TeV in order to reproduce the observed relic density. Moreover, the components of the MDM multiplet are always required to be nearly degenerate. This enhances the co-annihilation cross sections and also leads the Sommerfeld correction to the cross sections. Therefore this implies even heavier DM particles, with masses above 10 TeV [21, 33]. Even if the DM mass is below the W boson mass, efficient co-annihilation with the charged particles in the MDM multiplet is still at work, and the DM relic density would be too low.

In the absence of the heavy neutrinos, the above problem would be present in our models. However, the picture is slightly changed due to the non-thermal production of DM in the out-of-equilibrium decay of the right-handed neutrinos. The lightest right-handed neutrino is expected to be produced by a freeze-in mechanism in the early universe

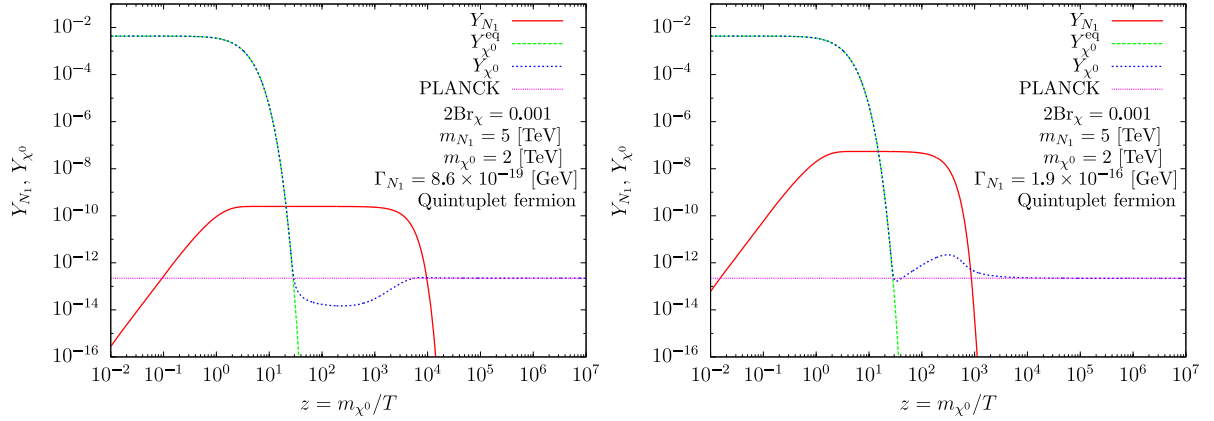


Figure 1: Examples of solutions of the coupled Boltzmann equations.

if its Yukawa couplings are small enough [34–38]. Then, once produced, it mainly decays into two body final states, $N_1 \rightarrow h\nu_\alpha, Z\nu_\alpha, W^\pm\ell_\alpha^\mp$. The decay width into two body final states is computed as

$$\Gamma_{N_1} = \frac{(y^\nu y^{\nu\dagger})_{11} m_{N_1}}{8\pi}, \quad (13)$$

where the masses of the gauge and Higgs bosons have been neglected.⁴ There are also subdominant three body N_1 decay processes into the components of the multiplet, such as $N_1 \rightarrow \chi^\pm\chi^\mp\nu_\alpha$ and $N_1 \rightarrow \chi^0\chi^\pm\ell_\alpha^\mp$, mediated by the gauge bosons. Then the charged particles decay into χ^0 . These three body decay processes occur due to the mixing between left-handed and right-handed neutrinos. The branching ratio of these processes, including all the components of the MDM multiplet, will be denoted as Br_χ . The number of DM particles produced per N_1 decay is 2Br_χ , since a pair of DM particles is produced in each decay of N_1 due to the conservation of the accidental \mathbb{Z}_2 parity. In our analysis we will consider Br_χ as a free parameter. Although the minimal models discussed in this paper predict a too low Br_χ value, we will comment below on how to increase this parameter with a minimal extension.

The evolution of the number densities of the N_1 and χ^0 species in the early universe is given by the coupled Boltzmann equations

$$\frac{dn_{N_1}}{dt} + 3Hn_{N_1} = \frac{g_{N_1}m_{N_1}^2m_{\chi^0}\Gamma_{N_1}}{2\pi^2z}K_1\left(\frac{m_{N_1}}{m_{\chi^0}}z\right) - \Gamma_{N_1}n_{N_1}, \quad (14)$$

$$\frac{dn_{\chi^0}}{dt} + 3Hn_{\chi^0} = -\langle\sigma_{\text{eff}}v\rangle\left(n_{\chi^0}^2 - n_{\chi^0}^{\text{eq}2}\right) + 2\text{Br}_\chi\Gamma_{N_1}n_{N_1}. \quad (15)$$

Here $z = m_{\chi^0}/T$ with the temperature of the universe T , $g_{N_1} = 2$ is the number of degrees of freedom of N_1 , $K_1(z)$ is the second modified Bessel function, $n_{\chi^0}^{\text{eq}}$ is the equilibrium num-

⁴Note that in order to simplify the notation we have decided to denote the N_1 decay width into two body final states as Γ_{N_1} . However, this should not be confused with the N_1 total decay width, which would also include three body final states.

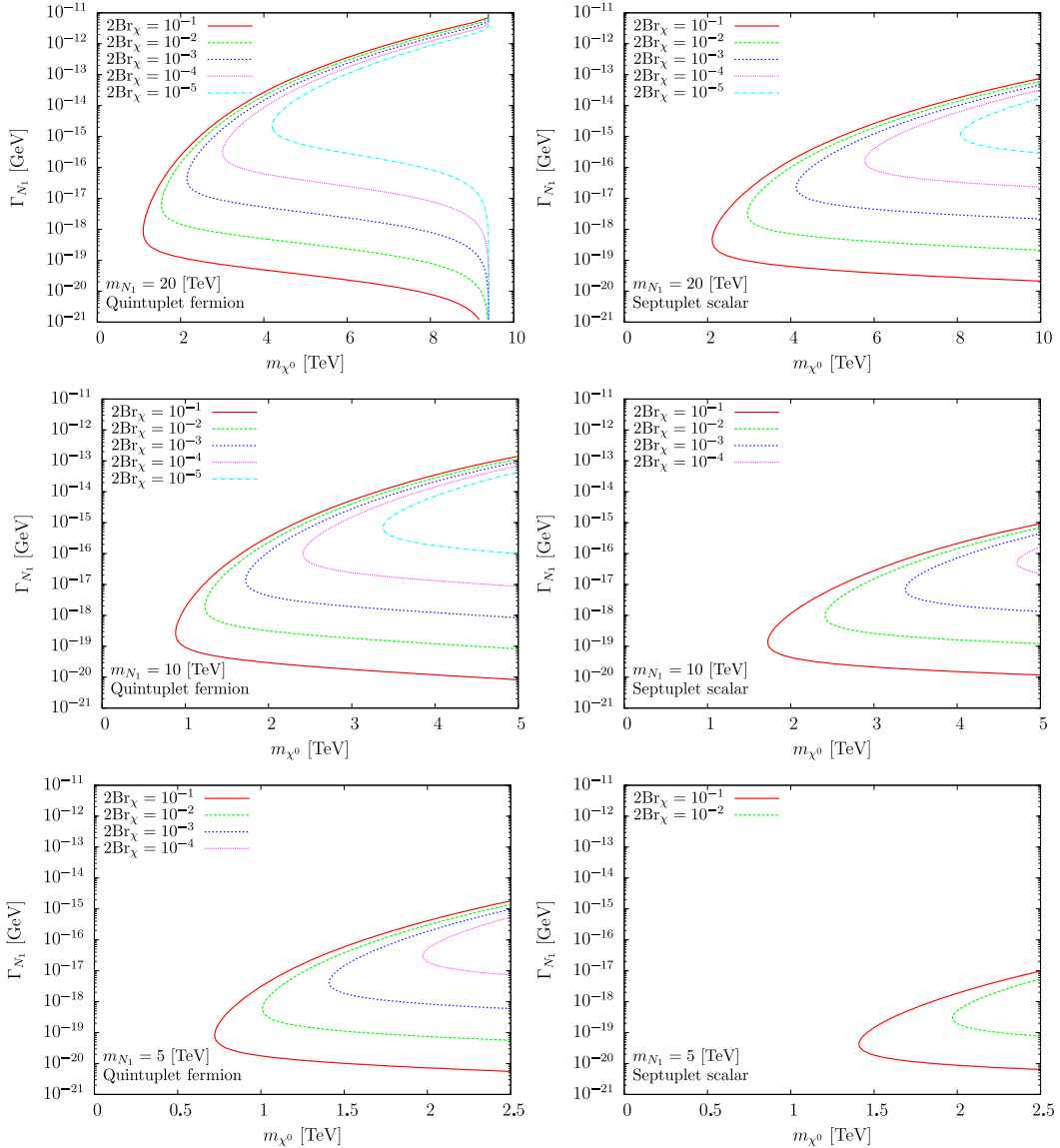


Figure 2: Contours satisfying the observed DM relic density in the m_{χ^0} - Γ_{N_1} plane for several fixed Br_{χ} . The lightest right-handed neutrino mass is fixed to $m_{N_1} = 20$ TeV for the upper panels, $m_{N_1} = 10$ TeV for the middle ones and $m_{N_1} = 5$ TeV for the bottom ones. The left panels are for the quintuplet fermion DM case while the right panels are for the septuplet scalar DM scenario.

ber density of χ^0 and $\langle\sigma_{\text{eff}}v\rangle$ is the thermally averaged effective DM annihilation cross section, including co-annihilation processes with degenerate particles. The dominant annihilation and co-annihilation channels are $\chi^0\chi^0 \rightarrow W^{\pm}W^{\mp}$ and $\chi^0\chi^{\pm}, \chi^{\mp}\chi^{\pm\pm} (\chi^{\mp\mp}\chi^{\pm\pm}) \rightarrow W^{\pm*} \rightarrow \gamma W^{\pm}$. In our analysis we approximately include the Sommerfeld effect for the effective annihilation cross section by using the results obtained in Ref. [21].

The DM relic density is obtained by solving the Boltzmann equations. For the nu-

merical analysis, it proves convenient to replace the number densities n_{N_1} and n_{χ^0} by $Y_{N_1} = n_{N_1}/s$ and $Y_{\chi^0} = n_{\chi^0}/s$, where s is the entropy density. Similarly, the time variable t is rewritten in terms of the temperature T . Some examples of numerical solutions are shown in Fig. 1, obtained for the quintuplet fermion DM scenario, with $2\text{Br}_\chi = 0.001$, $m_{N_1} = 5$ TeV and $m_{\chi^0} = 2$ TeV. For each fixed DM mass, two different values of the decay width Γ_{N_1} can satisfy the observed relic density. For a small decay width Γ_{N_1} , the amount of produced N_1 is moderate and they slowly decay after DM freeze-out (left panel in Fig. 1). For a large decay width Γ_{N_1} , a lot of N_1 's are created and they decay somewhat fast into DM particles (right panel in Fig. 1). In this case, since the DM particles are still coupled with the thermal bath, the DM production due to the decay of N_1 and the DM annihilation compete. The correct relic density is finally obtained.

The parameter space satisfying the DM relic density measured by Planck for several fixed values of Br_χ is shown in Fig. 2. One can see from the figure that for the quintuplet fermion scenario, the decay width of the lightest heavy neutrino Γ_{N_1} should satisfy

$$\begin{aligned} 10^{-18} \text{ GeV} &\lesssim \Gamma_{N_1} \lesssim 10^{-12} \text{ GeV} && \text{for } m_{N_1} = 20 \text{ TeV}, \\ 10^{-18} \text{ GeV} &\lesssim \Gamma_{N_1} \lesssim 10^{-13} \text{ GeV} && \text{for } m_{N_1} = 10 \text{ TeV}, \\ 10^{-18} \text{ GeV} &\lesssim \Gamma_{N_1} \lesssim 10^{-15} \text{ GeV} && \text{for } m_{N_1} = 5 \text{ TeV}, \end{aligned}$$

in order to get the measured DM relic density with $2\text{Br}_\chi \lesssim 0.001$. Thus, one finds that the required size of the lightest right-handed neutrino Yukawa coupling satisfies $10^{-11} \lesssim y^\nu \lesssim 10^{-8}$. For the septuplet scalar DM scenario, a larger branching ratio is required because the effective annihilation cross section is larger than in the quintuplet fermion DM case. In both cases we find that a much lower DM mass, compared to the standard MDM scenario, is possible. This is the main result of our paper.

A threshold at $m_{\chi^0} \approx 9.4$ TeV is observed in the upper left panel of Fig. 2. When the DM mass is above 9.4 TeV, the effective annihilation cross section becomes too small, leading to $\Omega_{\text{DM}} h^2 > 0.12$. Since the N_1 decay can only increase the DM relic density, the $m_{\chi^0} > 9.4$ TeV region is excluded in our scenario. One should also note that a lower bound on the decay width Γ_{N_1} can be derived from Big Bang Nucleosynthesis (BBN). The conservative bound for the N_1 lifetime $\tau_{N_1} \lesssim 0.1$ s, which corresponds to $\Gamma_{N_1} \gtrsim 10^{-23}$ GeV, should be taken into account not to affect the predictions of BBN [39, 40].⁵

Since the Yukawa coupling for the non-thermal production of DM is required to be rather small, the lightest heavy neutrino N_1 does not play any role in the generation of active neutrino masses. As a result of this, the active neutrino masses and mixings are explained by the other heavy neutrinos N_2 and N_3 , with the Yukawa couplings of the order of $y^\nu \sim 10^{-6}$.

⁵If the N_1 lifetime was longer than 10^3 s, the DM particles produced by the decay of N_1 would give an additional contribution to the number of effective neutrino species without affecting BBN. This is possible since the DM particles are relativistic due to their large kinetic energy [41]. However, this is not the case in our scenario, where the N_1 lifetime is shorter.

We briefly comment on DM particles lighter than the W boson mass. For DM masses below m_W , the DM relic density can be non-thermally produced with $2\text{Br}_\chi \gtrsim 0.01$ if the mass of the lightest right-handed neutrino is $m_{N_1} \lesssim 300$ GeV. However, there are two reasons to disregard this scenario. First, the required branching ratio into DM is too large and calls for an extension of the model, as explained below. And second, and more importantly, this DM mass range is completely excluded by the constraints from collider experiments as discussed in Sec. 4.1.

Getting the required Br_χ value

In the minimal models discussed in this paper one expects a small Br_χ value for $m_{\chi^0} \gg m_W, m_Z$. The main reason is intuitive: three body decays are suppressed compared to two body ones since the mediators of the three body decays, the W^\pm and Z gauge bosons, are much lighter than N_1 . In the septuplet scalar case, the Higgs boson can also mediate these decays via the scalar coupling $\lambda_{\phi\chi}$. However, the branching ratio Br_χ cannot be made as large as required to account for the DM relic density even if the maximum $\lambda_{\phi\chi}$ value allowed by direct detection experiments is considered.

This problem can be easily solved by adding a new heavy mediator for the three body decays. The simplest one would be a real scalar σ , with couplings to a pair of χ fields ($y_\sigma m_\chi \sigma \chi \chi$ or $y_\sigma \sigma \overline{\chi^c} \chi$ depending on the variant of the MDM scenario considered). The real scalar σ would mix with the SM Higgs boson h and, as a consequence of this, the lightest right-handed neutrino N_1 would decay into $N_1 \rightarrow \chi \overline{\chi} \nu_\alpha$. One should note that although the term $\sigma \overline{N_i^c} N_j$ is also possible, this coupling should be small enough so that N_1 is not in thermal equilibrium and can be produced by the freeze-in mechanism. We find that the required value of the $h - \sigma$ mixing angle is $\sin \alpha \sim 0.1$ and the mass of the new mediator (H , the heaviest mass eigenstate resulting from h and σ) is $m_H \gtrsim m_\chi$ for $y_\sigma = \mathcal{O}(0.1)$. The coupling y_σ is also constrained by DM direct detection experiments, and we have checked that the value $y_\sigma = \mathcal{O}(0.1)$ is consistent with the current LUX bound for TeV scale DM. We also have checked that the coupling $y_\sigma = \mathcal{O}(0.1)$ does not affect to the DM relic density and indirect detection, which will be discussed in the following section, since the electroweak interaction of the MDM multiplet is dominant. The required mixing angle is perfectly consistent with the current measurements of the Higgs properties by the LHC [42, 43]. Finally, such a real scalar could be related to the breaking of an extra symmetry existing at higher energy scales such as, for example, $U(1)_L$ or $U(1)_{B-L}$, where L and B are lepton and baryon numbers, respectively.

4 Constraints

In this section we review the most relevant constraints in our scenario. These come from collider searches as well as from dark matter indirect and direct detection experiments.

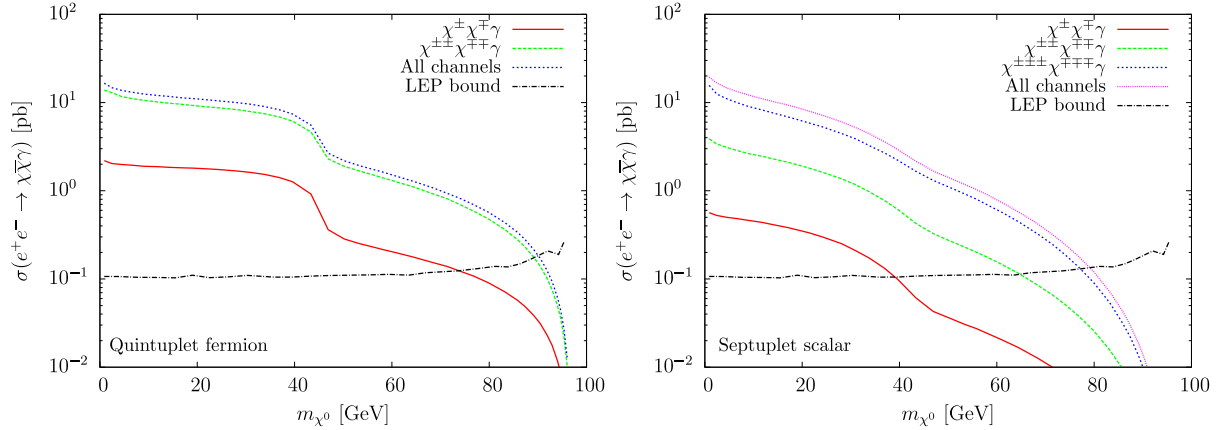


Figure 3: LEP limits on quintuplet fermion (left) and septuplet scalar (right) scenarios. In the derivation of these limits we have taken photon polar angles in the $46^\circ < \theta < 135^\circ$ range and photon energies $E_\gamma > 6$ GeV.

4.1 Collider constraints in low dark matter mass scenarios

Let us briefly comment on collider constraints in our scenario. These are of course only relevant for low dark matter masses and, as we will see, they strongly restrict this possibility.

First, we consider LEP bounds. Collider constraints derived from mono-photon searches at LEP turn out to be very strong for low dark matter masses. Multi-charged particles plus a photon are produced by the process

$$e^+e^- \rightarrow Z^*/\gamma^* \rightarrow \chi^\pm \chi^\mp \gamma, \chi^{\pm\pm} \chi^{\mp\mp} \gamma, \left(\chi^{\pm\pm\pm} \chi^{\mp\mp\mp} \gamma \right).$$

Then, the multi-charged particles decay into

$$\begin{aligned} \chi^\pm &\rightarrow \chi^0 W^{\pm*} \rightarrow \chi^0 \pi^\pm, \\ \chi^{\pm\pm} &\rightarrow \chi^0 W^{\pm*} W^{\pm*} \rightarrow \chi^0 \pi^\pm \pi^\pm, \\ \chi^{\pm\pm\pm} &\rightarrow \chi^0 W^{\pm*} W^{\pm*} W^{\pm*} \rightarrow \chi^0 \pi^\pm \pi^\pm \pi^\pm, \end{aligned}$$

producing soft pions due to the mass degeneracy among the components of the MDM multiplet χ . Therefore, if these pions are not seen due to their low energies, the resulting signal at LEP is mono-photon plus missing energy $e^+e^- \rightarrow \gamma \cancel{E}$. Using DELPHI data [44, 45], the authors of Ref. [46] used this idea to set limits on the suppression scale Λ of four-fermion contact interactions of the type $\mathcal{O}_4 \sim \frac{1}{\Lambda^2} \bar{\chi} \chi \bar{e} e$.

Here, we translate the lower limits of the suppression scale Λ into upper limits on the total production cross section for $e^+e^- \rightarrow \chi \bar{\chi} \gamma$, where χ denotes χ^\pm , $\chi^{\pm\pm}$ ($\chi^{\pm\pm\pm}$). Although the energy distribution of the mono-photon in our case is not exactly the same as that obtained with the contact interactions, this estimate should provide a rough limit

in our scenario. For our analysis we consider photons with polar angles θ in the range $45^\circ < \theta < 135^\circ$ and energies $E_\gamma > 6$ GeV. These kinematical cuts are required to be consistent with the detection capabilities of the High Density Projection Chamber of DELPHI. Our results are shown in Fig. 3, both for the quintuplet fermion and septuplet scalar. As one can see from the figures, a slightly stronger constraint is obtained for the quintuplet fermion. DM masses $m_{\chi^0} \lesssim 90$ GeV for the quintuplet fermion and $m_{\chi^0} \lesssim 79$ GeV for the septuplet scalar are excluded. We point out that very similar bounds have been obtained in the recent Ref. [30].

Regarding LHC bounds, these have been recently analyzed in [47]. For the quintuplet fermion case, the lower bound $m_{\chi^0} \gtrsim 267$ GeV has been obtained with the LHC running at $\sqrt{s} = 8$ TeV and 20.3 fb^{-1} of integrated luminosity in ATLAS and 19.5 fb^{-1} in CMS [47]. This bound will be improved up to $m_{\chi^0} \gtrsim 668$ GeV if the LHC does not find a signal with $\sqrt{s} = 14$ TeV and 3 ab^{-1} .

4.2 Gamma-ray constraints

The DM annihilation channels $\chi^0\chi^0 \rightarrow W^+W^-$ and $\chi^0\chi^0 \rightarrow \gamma\gamma$ induce indirect detection signals of DM. At present time, the cross sections for these two annihilation processes are drastically affected by the non-perturbative Sommerfeld effect due to the low kinetic energy of the DM particles. This typically leads to relevant constraints from observations of gamma-rays coming from dwarf spheroidal satellite galaxies or the galactic center [48, 49]. Note that even for the W^+W^- annihilation channel, high energy gamma-rays are generated in the decay of the W boson.

Let us elaborate on the so-called Sommerfeld effect. As we have already discussed, the components of the MDM multiplets are naturally degenerate, and the mass scale of the DM particles is much higher than that of the gauge boson masses. In this case, the usual perturbative calculation for annihilation cross sections is not valid because long-range Coulomb-like forces which imply the Yukawa forces with small mediator masses among the MDM components distort the plane wave function of the incoming DM two-body state. Hence, the annihilation cross sections must be calculated non-perturbatively by taking into account the Sommerfeld correction [50]. This was pointed out for the first time for a wino-like neutralino DM scenario in supersymmetric models [33, 51–54]. A similar calculation was performed for MDM models in Ref. [21]. In our models, the calculation is basically the same, except for the mass range we focus on. Therefore, we must proceed to the re-evaluation of the Sommerfeld enhanced cross sections, in order to be able to compare to the current bounds from indirect detection experiments.

Our numerical analysis follows Ref. [55] and includes only the s -wave component of the cross section. In order to obtain the correction factor for the amplitude induced by the Sommerfeld effect, we must solve a coupled Schrödinger equation in the presence of a

potential generated by long-range forces,

$$-\frac{1}{m_{\chi^0}} \frac{d^2 \psi_i}{dr^2} + V_{ij} \psi_j = \frac{m_{\chi^0} v^2}{4} \psi_i, \quad (16)$$

where ψ_i is the wave function of the two-body DM state and V_{ij} is the potential matrix. The indices i, j run as $i, j = 1 - 3$ for the quintuplet fermion and as $i, j = 1 - 4$ for the septuplet scalar. The wave function ψ and the potential matrix V are explicitly given by

$$\psi = \begin{pmatrix} \langle r | \chi^{++} \chi^{--} \rangle \\ \langle r | \chi^+ \chi^- \rangle \\ \langle r | \chi^0 \chi^0 \rangle \end{pmatrix}, \quad V = \begin{pmatrix} 8\Delta - 4A & -2B & 0 \\ -2B & 2\Delta - A & -3\sqrt{2}B \\ 0 & -3\sqrt{2}B & 0 \end{pmatrix}, \quad (17)$$

for the quintuplet fermion and

$$\psi = \begin{pmatrix} \langle r | \chi^{+++} \chi^{---} \rangle \\ \langle r | \chi^{++} \chi^{--} \rangle \\ \langle r | \chi^+ \chi^- \rangle \\ \langle r | \chi^0 \chi^0 \rangle \end{pmatrix}, \quad V = \begin{pmatrix} 18\Delta - 9A & -3B & 0 & 0 \\ -3B & 8\Delta - 4A & -5B & 0 \\ 0 & -5B & 2\Delta - A & -6\sqrt{2}B \\ 0 & 0 & -6\sqrt{2}B & 0 \end{pmatrix}, \quad (18)$$

for the septuplet scalar. Here $A = \alpha_{\text{em}}/r + \alpha_W \cos^2 \theta_W e^{-m_Z r}/r$, $B = \alpha_W e^{-m_W r}/r$, $\Delta = 166$ MeV and r is the distance between the two DM particles. The non-trivial factor $\sqrt{2}$ appears in some matrix elements of the potential due to the different normalization between the neutral and charged states.

We are interested in the annihilation of the neutral state, which is governed by physics at short distances and thus described by the wave function at the origin, $\psi(0)$. Therefore, as discussed in Refs. [21, 55, 56], in order to evaluate the Sommerfeld correction factor, we must solve the Schrödinger equation with linear independent boundary conditions for irregular solutions at the origin. For the quintuplet fermion, these boundary conditions at the origin and at $r \rightarrow \infty$ are explicitly given by

$$\psi(0) = \begin{pmatrix} 1 \\ 0 \\ 0 \end{pmatrix}, \quad \begin{pmatrix} 0 \\ 1 \\ 0 \end{pmatrix}, \quad \begin{pmatrix} 0 \\ 0 \\ 1 \end{pmatrix}, \quad \frac{d\psi(\infty)}{dr} = \begin{pmatrix} ik_1 & 0 & 0 \\ 0 & ik_2 & 0 \\ 0 & 0 & ik_3 \end{pmatrix} \psi(\infty), \quad (19)$$

where $k_i \equiv \sqrt{m_{\chi^0}^2 v^2 - m_{\chi^0} V_{ii}(\infty)}/2$. After solving the Schrödinger equation for each boundary condition at the origin, the Sommerfeld factor matrix A_{ij} is given by

$$A_{ij} = \psi_i^{(j)}(r) e^{-ik_i r} \Big|_{r \rightarrow \infty}, \quad (20)$$

where the superscript j implies j -th boundary condition. The above discussion is straightforwardly extended to the septuplet scalar.

Finally, the absorptive parts describing the DM annihilations for the W^+W^- and $\gamma\gamma$ channels are given by

$$\Gamma_{WW} = \frac{\pi \alpha_W^2}{m_{\chi^0}^2} \begin{pmatrix} 2 & 5 & 3\sqrt{2} \\ 5 & 25/2 & 15/\sqrt{2} \\ 3\sqrt{2} & 15/\sqrt{2} & 9 \end{pmatrix}, \quad \Gamma_{\gamma\gamma} = \frac{\pi \alpha_{\text{em}}^2}{m_{\chi^0}^2} \begin{pmatrix} 16 & 4 & 0 \\ 4 & 1 & 0 \\ 0 & 0 & 0 \end{pmatrix}, \quad (21)$$

for the quintuplet fermion and

$$\Gamma_{WW} = \frac{\pi\alpha_W^2}{m_{\chi^0}^2} \begin{pmatrix} 9 & 24 & 33 & 18\sqrt{2} \\ 24 & 64 & 88 & 48\sqrt{2} \\ 33 & 88 & 121 & 66\sqrt{2} \\ 18\sqrt{2} & 48\sqrt{2} & 66\sqrt{2} & 72 \end{pmatrix}, \quad \Gamma_{\gamma\gamma} = \frac{2\pi\alpha_{\text{em}}^2}{m_{\chi^0}^2} \begin{pmatrix} 81 & 36 & 9 & 0 \\ 36 & 16 & 4 & 0 \\ 9 & 4 & 1 & 0 \\ 0 & 0 & 0 & 0 \end{pmatrix}, \quad (22)$$

for the septuplet scalar. The DM annihilation cross sections can be computed from the absorptive parts and the Sommerfeld factor A as

$$\sigma v_{WW} = 2 (A\Gamma_{WW}A^\dagger)_{33}, \quad \sigma v_{\gamma\gamma} = 2 (A\Gamma_{\gamma\gamma}A^\dagger)_{33}, \quad (23)$$

for the quintuplet fermion and

$$\sigma v_{WW} = 2 (A\Gamma_{WW}A^\dagger)_{44}, \quad \sigma v_{\gamma\gamma} = 2 (A\Gamma_{\gamma\gamma}A^\dagger)_{44}, \quad (24)$$

for the septuplet scalar.

Our numerical results for the quintuplet fermion and septuplet scalar into W^+W^- and $\gamma\gamma$ are shown in Fig. 4. The DM relative velocity is fixed to $v = 10^{-3}$. Since the actual DM velocity has a distribution, the cross section should be averaged over the DM velocity in a more sophisticated analysis. For the W^+W^- channel, the upper bound on gamma-ray observations coming from dwarf spheroidal galaxies (assuming NFW profile) is also shown [48]. For the $\gamma\gamma$ channel, the blue points show the H.E.S.S. limit for monochromatic gamma-ray lines coming from the galactic centre, assuming in this case a Einasto profile [49]. As one can see from the figures, the cross sections largely exceed the bounds except in several dips. These dips can be interpreted in analogy with the Ramsauer-Townsend effect, the scattering of low energy electrons by atoms of a noble gas [57, 58]. The Ramsauer-Townsend effect is caused by the electromagnetic interaction, and the positions of the dips strongly depend on the mass difference Δ [57, 58]. Due to this effect, the incoming two DM particles pass through unaffected by the potential when the DM pair has a fixed energy, thus drastically decreasing the annihilation cross section. When the mass difference Δ is as large as $\mathcal{O}(10)$ GeV, the dips tends to disappear since the electromagnetic transition between the DM and the charged states becomes unefficient. The resonant behaviour in Fig. 4 is caused by the bound state of the two DM particles with zero binding energy [52, 53, 57, 58].

For the quintuplet fermion, the dips appear at DM masses around 2 TeV and 7.5 TeV for the W^+W^- channel. The positions of the dips are very close to those in the $\gamma\gamma$ channel. This is the only possibility to evade the gamma-ray constraints simultaneously for W^+W^- and $\gamma\gamma$ final states. For the septuplet scalar, the same thing occurs at around 5.5 TeV and 7 TeV.

Note that the gamma-ray constraints depend on DM profiles. If a cored DM profile such as Burkert or Isothermal is assumed, these constraints are relaxed. Concerning this uncertainty, two orders of magnitude looser bounds are expected at most. Moreover since

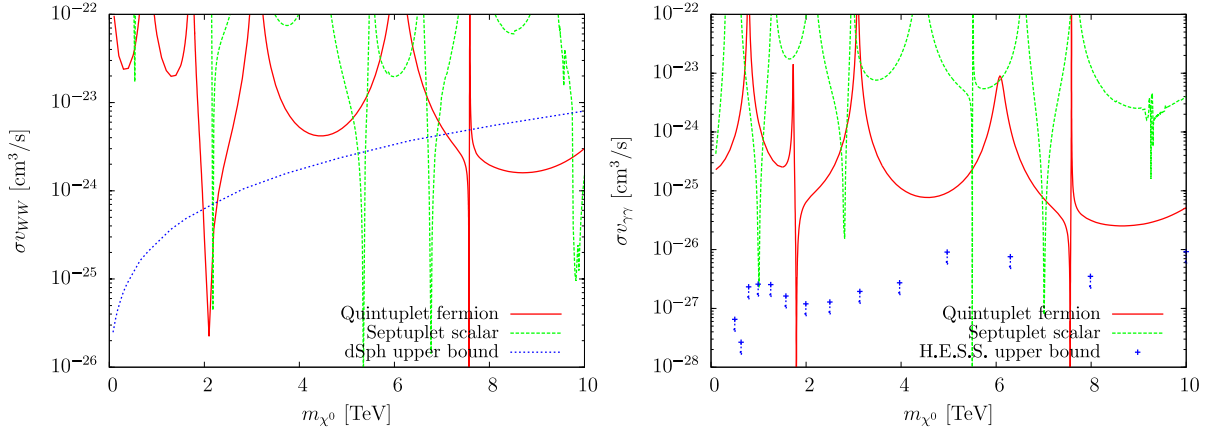


Figure 4: Cross sections for $\chi^0\chi^0 \rightarrow W^+W^-$ and $\chi^0\chi^0 \rightarrow \gamma\gamma$. The DM relative velocity is fixed to $v = 10^{-3}$.

the positions of the dips due to the Ramsauer-Townsend strongly depend on the mass difference Δ , if a larger mass difference, like $\mathcal{O}(1)$ GeV, were possible by an extension of the model, a broader DM mass range would be able to satisfy the gamma-ray constraints.

We point out that for the septuplet scalar DM, there are additional contributions to the annihilations into W^+W^- and $\gamma\gamma$ due to the scalar couplings $\lambda_{\phi\chi}$ and λ_χ . These contributions would lead to an increase. However, they are found to be subdominant compared to the gauge boson loops (with the Sommerfeld correction calculated above).

One should note that the above discussion of the dips due to the Ramsauer-Townsend effect is controversial. More detailed analyses have recently been done in Refs. [59, 60]. According to these references, in addition to the W^+W^- and $\gamma\gamma$ channels, gamma-ray production in the ZZ , $Z\gamma$ and $W^+W^-\gamma$ channels should also be taken into account. If these channels are included, the dips disappear and thermally produced MDM with a mass $m_{\chi^0} \approx 9.4$ TeV for the quintuplet fermion or $m_{\chi^0} \approx 25$ TeV for the septuplet scalar is excluded in the case of cusp DM profiles such as NFW and Einasto, but still allowed for cored profiles like Isothermal.⁶ For lower DM masses, as in our case, the gamma-ray constraint becomes stronger than in the thermal MDM scenario. There is, however, a valid region in the parameter space (with a specific DM mass) when cored DM profiles are considered.

4.3 Direct detection

In the MDM scenario, elastic scattering with quarks is induced at the one-loop level via $SU(2)_L$ gauge interactions. Our setup with non-thermal DM production allows for lighter DM particles than in the in the standard MDM scenario with thermally produced DM. With non-thermal production we find valid DM masses below 7.5 TeV in both cases,

⁶Another way to evade the gamma-ray constraint would be to assume a sub-dominant MDM scenario.

whereas in the standard thermal scenario one has 9.4 TeV for the quintuplet fermion and 25 TeV for the septuplet scalar. For this reason, we expect that the constraints derived from direct detection experiments will be stronger than those obtained in the usual thermal scenario.

The one-loop spin independent elastic cross section with a proton was found in Ref. [9] to be about $\sigma_p \sim 10^{-44} \text{ cm}^2$. This value for the cross section may seem too large compared to the current experimental bound obtained by LUX for a DM mass $m_{\chi^0} \lesssim 7.5 \text{ TeV}$. However, according to recent calculations including two-loop diagrams including DM and gluons, the Higgs mass measured at the LHC and recent lattice simulations for the strangeness content of the nucleon, it turns out that the elastic cross section gets reduced due to partial cancellations, leading to $\sigma_p \sim 10^{-46} \text{ cm}^2$ [61,62]. This is below the current LUX bound and testable by the future direct detection experiments such as XENON1T. Given that the DM particles in our scenario are lighter than those present in scenarios with thermally produced MDM, the coming direct detection experiments will also test our setup.

5 Summary and Conclusions

In this paper we have discussed an extension of the SM with three right-handed neutrinos and a large $SU(2)_L$ multiplet. The $SU(2)_L$ multiplet is either a quintuplet fermion or a septuplet scalar. Despite imposing no additional symmetry, the lightest neutral component of the multiplet can constitute the DM content of the universe because of an accidental symmetry, as in the conventional MDM scenario. Furthermore, neutrino masses are induced by the canonical Type-I seesaw mechanism.

However, unlike the conventional MDM scenario with thermally produced DM, in our setup the DM particles are non-thermally produced by the decay of the heavy neutrinos. This allows to lower significantly the DM mass and still be compatible with the observed DM relic density. Instead of DM masses as large as 9.4 TeV or 25 TeV, the DM mass in our non-thermal scenario can be as light as a few TeV.

Finally, we have considered several experimental constraints in our scenario. First, we have discussed the possibility of a DM mass below the W boson mass, which is excluded due to strong constraints coming from mono-photon plus missing energy searches at LEP. In particular, we found that the mass ranges $m_{\chi^0} \lesssim 90 \text{ GeV}$ and $m_{\chi^0} \lesssim 79 \text{ GeV}$ are excluded for the quintuplet fermion and septuplet scalar cases, respectively. Next, we considered indirect detection constraints, especially relevant due to potentially large Sommerfeld enhancements. In fact, we found that the annihilation cross sections for the W^+W^- and $\gamma\gamma$ channels are considerably affected by the Sommerfeld effect. The quintuplet fermion DM can evade the strong constraints of the gamma-ray experiments at around only $m_{\chi^0} \approx 2 \text{ TeV}$ and 7.5 TeV due to the drastic decrease of the cross sections by the Ramsauer-Townsend effect. For the septuplet scalar DM, the same thing occurs and the DM is predicted to be $m_{\chi^0} \approx 5.5 \text{ TeV}$ or 7 TeV . In addition, if more detailed

analyses of the gamma-ray constraints in MDM scenarios are taken into account, our scenario would be allowed only at specific DM masses for cored DM profiles.

Acknowledgments

The authors would like to thank Asmaa Abada, Marco Cirelli, Renato M. Fonseca, Koichi Hamaguchi, Filippo Sala and Marco Taoso for fruitful discussions and Florian Staub for assistance in the implementation of septuplets in SARAH [63]. The work of M. A. is supported in part by the Japan Society for the Promotion of Sciences (JSPS) Grant-in-Aid for Scientific Research (Grant No. 25400250 and No. 26105509). T. T. acknowledges support from the European ITN project (FP7-PEOPLE-2011-ITN, PITN-GA-2011-289442-INVISIBLES) and P2IO Excellence Laboratory. Numerical computation in this work was carried out at the Yukawa Institute Computer Facility. This research was partially supported by the Munich Institute for Astro- and Particle Physics (MIAPP) of the DFG cluster of excellence ‘‘Origin and Structure of the Universe’’.

A $SU(2)$ Multiplet Notation

There are two common ways to denote $SU(2)$ multiplets:

- **Tensor notation:** This is the usual choice, see Refs. [28, 29]. A multiplet Φ would be represented by a symmetric tensor with some indices, (four indices for quintuplet Φ^{ijkl} and six indices for septuplet Φ^{ijklmn}), where all indices can take values 1 or 2.
- **Vector notation:** This is the choice made in this paper. In this case, the quintuplet and septuplet are simply represented by a vector of 5 and 7 elements.

Since both notations are equally correct, this choice is just a matter of taste. In fact, a *dictionary* that translates the analytical expressions among notations can be easily found. Regarding the elements of the quintuplet and septuplet, the relation between the two notations is given by

$$\Phi^{ijkl} \equiv i \begin{pmatrix} +\Phi^{1111} \\ +2\Phi^{1112} \\ -\sqrt{6}\Phi^{1122} \\ +2\Phi^{1222} \\ +\Phi^{2222} \end{pmatrix}, \quad \Phi^{ijklmn} \equiv i \begin{pmatrix} +\Phi^{11111} \\ +\sqrt{6}\Phi^{11112} \\ +\sqrt{15}\Phi^{11122} \\ -\sqrt{20}\Phi^{11222} \\ -\sqrt{15}\Phi^{12222} \\ +\sqrt{6}\Phi^{12222} \\ -\Phi^{22222} \end{pmatrix}. \quad (25)$$

This allows us to write the quintuplet and septuplet χ as shown in Eq. (1).

We now comment on $SU(2)$ septuplet direct products. The product $\mathbf{7} \otimes \mathbf{7}$ can be decomposed as

$$\mathbf{7} \otimes \mathbf{7} = \mathbf{13}_S \oplus \mathbf{11}_A \oplus \mathbf{9}_S \oplus \mathbf{7}_A \oplus \mathbf{5}_S \oplus \mathbf{3}_A \oplus \mathbf{1}_S, \quad (26)$$

where the indices S and A mean symmetric and anti-symmetric contractions. The symmetry properties of septuplet contractions are fundamental in order to determine the number of relevant scalar couplings. For example, when one considers χ^4 , four kinds of singlets are obtained since anti-symmetric parts vanish:⁷

$$\begin{aligned}
& \mathbf{7} \otimes \mathbf{7} \otimes \mathbf{7} \otimes \mathbf{7} \\
&= (\mathbf{13} \oplus \mathbf{9} \oplus \mathbf{5} \oplus \mathbf{1}) \otimes (\mathbf{13} \oplus \mathbf{9} \oplus \mathbf{5} \oplus \mathbf{1}) \\
&\supset \mathbf{1} \oplus \mathbf{1}' \oplus \mathbf{1}'' \oplus \mathbf{1}'''.
\end{aligned} \tag{27}$$

However one can check that only two of them are linearly independent.

References

- [1] M. Lindner, D. Schmidt and T. Schwetz, Phys. Lett. B **705**, 324 (2011) [[arXiv:1105.4626](#) [hep-ph]].
- [2] S. Baek, H. Okada and T. Toma, JCAP **1406**, 027 (2014) [[arXiv:1312.3761](#) [hep-ph]].
- [3] N. Bernal, C. Garcia-Cely and R. Rosenfeld, [arXiv:1501.01973](#) [hep-ph].
- [4] T. Hambye, JHEP **0901**, 028 (2009) [[arXiv:0811.0172](#) [hep-ph]].
- [5] P. Ko and Y. Tang, JCAP **1405**, 047 (2014) [[arXiv:1402.6449](#) [hep-ph], [arXiv:1402.6449](#)].
- [6] S. Baek, P. Ko and W. I. Park, Phys. Lett. B **747**, 255 (2015) [[arXiv:1407.6588](#) [hep-ph]].
- [7] M. Hirsch, S. Morisi, E. Peinado and J. W. F. Valle, Phys. Rev. D **82** (2010) 116003 [[arXiv:1007.0871](#) [hep-ph]].
- [8] S. D. Aristizabal, M. Dhen, C. S. Fong and A. Vicente, Phys. Rev. D **91** (2015) 9, 096004 [[arXiv:1412.5600](#) [hep-ph]].
- [9] M. Cirelli, N. Fornengo and A. Strumia, Nucl. Phys. B **753**, 178 (2006) [[hep-ph/0512090](#)].
- [10] C. Q. Geng, L. H. Tsai and Y. Yu, [arXiv:1411.6344](#) [hep-ph].
- [11] Y. Yu, C. X. Yue and S. Yang, Phys. Rev. D **91**, no. 9, 093003 (2015) [[arXiv:1502.02801](#) [hep-ph]].
- [12] P. Culjak, K. Kumericki and I. Picek, Phys. Lett. B **744**, 237 (2015) [[arXiv:1502.07887](#) [hep-ph]].
- [13] K. Harigaya, K. Ichikawa, A. Kundu, S. Matsumoto and S. Shirai, [arXiv:1504.03402](#) [hep-ph].

⁷In principle, when more than one singlet can be obtained for a specific Lagrangian term, one must check whether they are linearly independent in order to avoid the introduction of redundant couplings.

- [14] A. Ahriche, K. L. McDonald, S. Nasri and T. Toma, Phys. Lett. B **746**, 430 (2015) [[arXiv:1504.05755](#) [hep-ph]].
- [15] M. Cirelli and A. Strumia, New J. Phys. **11** (2009) 105005 [[arXiv:0903.3381](#) [hep-ph]].
- [16] T. Hambye, F.-S. Ling, L. Lopez Honorez and J. Rocher, JHEP **0907** (2009) 090 [Erratum-ibid. **1005** (2010) 066] [[arXiv:0903.4010](#) [hep-ph]].
- [17] Y. Cai, W. Chao and S. Yang, JHEP **1212** (2012) 043 [[arXiv:1208.3949](#) [hep-ph]].
- [18] K. Earl, K. Hartling, H. E. Logan and T. Pilkington, Phys. Rev. D **88** (2013) 015002 [[arXiv:1303.1244](#) [hep-ph]].
- [19] J. M. Cline, K. Kainulainen, P. Scott and C. Weniger, Phys. Rev. D **88** (2013) 055025 [[arXiv:1306.4710](#) [hep-ph]].
- [20] R. Adam *et al.* [Planck Collaboration], [arXiv:1502.01582](#) [astro-ph.CO].
- [21] M. Cirelli, A. Strumia and M. Tamburini, Nucl. Phys. B **787**, 152 (2007) [[arXiv:0706.4071](#) [hep-ph]].
- [22] P. Minkowski, Phys. Lett. B **67** (1977) 421.
- [23] T. Yanagida, in *KEK lectures*, ed. O. Sawada and A. Sugamoto, KEK, 1979; M Gell-Mann, P Ramond, R. Slansky, in *Supergravity*, ed. P. van Nieuwenhuizen and D. Freedman (North Holland, 1979).
- [24] R. N. Mohapatra and G. Senjanovic, Phys. Rev. Lett. **44** (1980) 912.
- [25] J. Schechter and J. W. F. Valle, Phys. Rev. D **22**, 2227 (1980).
- [26] J. Schechter and J. W. F. Valle, Phys. Rev. D **25** (1982) 774.
- [27] T. Moroi, M. Nagai and M. Takimoto, JHEP **1307**, 066 (2013) [[arXiv:1303.0948](#) [hep-ph]].
- [28] J. Hisano and K. Tsumura, Phys. Rev. D **87**, no. 5, 053004 (2013) [[arXiv:1301.6455](#) [hep-ph]].
- [29] C. Alvarado, L. Lehman and B. Ostdiek, JHEP **1405**, 150 (2014) [[arXiv:1404.3208](#) [hep-ph]].
- [30] L. Di Luzio, R. Grober, J. F. Kamenik and M. Nardecchia, [arXiv:1504.00359](#) [hep-ph].
- [31] M. Ibe, S. Matsumoto and R. Sato, Phys. Lett. B **721**, 252 (2013) [[arXiv:1212.5989](#) [hep-ph]].
- [32] J. A. Casas and A. Ibarra, Nucl. Phys. B **618** (2001) 171 [[hep-ph/0103065](#)].
- [33] J. Hisano, S. Matsumoto, M. Nagai, O. Saito and M. Senami, Phys. Lett. B **646**, 34 (2007) [[hep-ph/0610249](#)].
- [34] J. McDonald, Phys. Rev. Lett. **88**, 091304 (2002) [[hep-ph/0106249](#)].

- [35] L. J. Hall, K. Jedamzik, J. March-Russell and S. M. West, JHEP **1003**, 080 (2010) [[arXiv:0911.1120](#) [hep-ph]].
- [36] M. Blennow, E. Fernandez-Martinez and B. Zaldivar, JCAP **1401**, no. 01, 003 (2014) [[arXiv:1309.7348](#) [hep-ph]].
- [37] M. Klasen and C. E. Yaguna, JCAP **1311** (2013) 039 [[arXiv:1309.2777](#) [hep-ph]].
- [38] E. Molinaro, C. E. Yaguna and O. Zapata, JCAP **1407**, 015 (2014) [[arXiv:1405.1259](#) [hep-ph]].
- [39] M. Kawasaki, K. Kohri and T. Moroi, Phys. Rev. D **71**, 083502 (2005) [[astro-ph/0408426](#)].
- [40] K. Jedamzik, Phys. Rev. D **74**, 103509 (2006) [[hep-ph/0604251](#)].
- [41] D. Hooper, F. S. Queiroz and N. Y. Gnedin, Phys. Rev. D **85**, 063513 (2012) [[arXiv:1111.6599](#) [astro-ph.CO]].
- [42] T. Robens and T. Stefaniak, Eur. Phys. J. C **75**, no. 3, 104 (2015) [[arXiv:1501.02234](#) [hep-ph]].
- [43] C. Bonilla, J. W. F. Valle and J. C. Romão, Phys. Rev. D **91** (2015) 113015 [[arXiv:1502.01649](#) [hep-ph]].
- [44] J. Abdallah *et al.* [DELPHI Collaboration], Eur. Phys. J. C **38**, 395 (2005) [[hep-ex/0406019](#)].
- [45] J. Abdallah *et al.* [DELPHI Collaboration], Eur. Phys. J. C **60**, 17 (2009) [[arXiv:0901.4486](#) [hep-ex]].
- [46] P. J. Fox, R. Harnik, J. Kopp and Y. Tsai, Phys. Rev. D **84**, 014028 (2011) [[arXiv:1103.0240](#) [hep-ph]].
- [47] B. Ostdiek, [arXiv:1506.03445](#) [hep-ph].
- [48] M. Ackermann *et al.* [Fermi-LAT Collaboration], [arXiv:1503.02641](#) [astro-ph.HE].
- [49] A. Abramowski *et al.* [HESS Collaboration], Phys. Rev. Lett. **110**, 041301 (2013) [[arXiv:1301.1173](#) [astro-ph.HE]].
- [50] A. Sommerfeld, Annalen der Physik, 403, 257 (1931).
- [51] J. Hisano, S. Matsumoto and M. M. Nojiri, Phys. Rev. D **67**, 075014 (2003) [[hep-ph/0212022](#)].
- [52] J. Hisano, S. Matsumoto and M. M. Nojiri, Phys. Rev. Lett. **92**, 031303 (2004) [[hep-ph/0307216](#)].
- [53] J. Hisano, S. Matsumoto, M. M. Nojiri and O. Saito, Phys. Rev. D **71**, 063528 (2005) [[hep-ph/0412403](#)].
- [54] J. Hisano, S. Matsumoto, O. Saito and M. Senami, Phys. Rev. D **73**, 055004 (2006) [[hep-ph/0511118](#)].

- [55] M. Baumgart, I. Z. Rothstein and V. Vaidya, JHEP **1504**, 106 (2015) [[arXiv:1412.8698](#) [hep-ph]].
- [56] N. Arkani-Hamed, D. P. Finkbeiner, T. R. Slatyer and N. Weiner, Phys. Rev. D **79**, 015014 (2009) [[arXiv:0810.0713](#) [hep-ph]].
- [57] E. J. Chun, J. C. Park and S. Scopel, JCAP **1212**, 022 (2012) [[arXiv:1210.6104](#) [astro-ph.CO]].
- [58] E. J. Chun and J. C. Park, [arXiv:1506.07522](#) [hep-ph].
- [59] M. Cirelli, T. Hambye, P. Panci, F. Sala and M. Taoso, [arXiv:1507.05519](#) [hep-ph].
- [60] C. Garcia-Cely, A. Ibarra, A. S. Lamperstorfer and M. H. G. Tytgat, [arXiv:1507.05536](#) [hep-ph].
- [61] M. Farina, D. Pappadopulo and A. Strumia, JHEP **1308**, 022 (2013) [[arXiv:1303.7244](#) [hep-ph]].
- [62] J. Hisano, K. Ishiwata and N. Nagata, [arXiv:1504.00915](#) [hep-ph].
- [63] F. Staub, Comput. Phys. Commun. **185** (2014) 1773 [[arXiv:1309.7223](#) [hep-ph]].